Inorg. Chem. **2004**, *43*, 4012–4018

Bonding in Tetrahedral $Cu_4(\mu_3\text{-}X)_4L_4$ Copper(I) Clusters: A DFT Investigation†

Andrés Vega‡,§,|| and Jean-Yves Saillard*,‡

Laboratoire de Chimie du Solide et Inorganique Moléculaire, UMR-CNRS 6511, Institut de Chimie de Rennes, Université de Rennes 1, 35042 Rennes Cedex, France, and Centro para la Investigación Interdisciplinaria Avanzada en Ciencia de los Materiales, Facultad de Ciencias Físicas y Matemáticas, Casilla 487-3, Universidad de Chile, Santiago, Chile

Received October 31, 2003

DFT calculations on $Cu_4(\mu_3\text{-}X)_4L_4$ (X = H, CH_3, CCH, F, Cl, Br, I; L = NH_3, PH_3) indicate that, regardless of its nature, X^- acts essentially as a two-electron σ-type ligand and that the covalent part of the Cu···Cu bonding depends mainly upon the a_1 component of the orbital interaction between the $L_4Cu_4^{4+}$ and X_4^{4-} fragments. The first excited state corresponds to the occupation of a Cu···Cu bonding LUMO of a_1 symmetry, which is of dominant Cu(4s/4p) character when X^- is an electronegative ligand, such as a halide. Consequently, this excited state is computed to exhibit Cu···Cu distances shorter than those in the ground state, in agreement with the luminescence properties of this type of compound.

Introduction

Copper(I) is known for its ability to form, in association with various types of bridging and terminal ligands, polynuclear (cluster) species of various shapes and sizes where weak bonding interactions between the closed-shell metal centers are generally present.[1] The nature of this d^{10}/d^{10} bonding has been debated for a long time in the literature. Extended Hückel calculations by Mehrotra and Hoffmann have shown the importance of the mixing of empty bonding combinations of 4s/4p atomic orbitals (AOs) into the occupied 3d-block.[2] Later, the significant role of electron correlation in this type of closed-shell/closed-shell interaction was also pointed out by Pyykko.[3] We have recently analyzed the bonding in various types of Cu(I) clusters by means of density functional theory (DFT) calculations.[4] In particular, our study on $Cu_4(\mu_2\text{-}Cl)_4(bipyridine)_2$ suggests that Cu···Cu distances are subjected not only to bridging ligand size or steric effects but also to the number of electrons given by the ligands to the Cu(I) centers.[4c] From this point of view, the large family of the tetrahedral cubane-like copper(I) complexes $Cu_4(\mu_3\text{-}X)_4L_4$ (L = two-electron ligand, X^- = two-electron or six-electron ligand) sketched in Figure 1 offers the possibility for analyzing the effect of electron count on a quite simple and symmetrical Cu_4 cluster core. Moreover, this type of compounds has attracted a large interest due to their rich photophysical properties.[5]

This paper reports DFT calculations on the model series $Cu_4(\mu_3\text{-}X)_4L_4$ (X = H, CH_3, CCH, F, Cl, Br, I; L = NH_3, PH_3). The bonding in these compounds is analyzed with respect to the nature and electron count of L and X, and a contribution to the understanding of the photophysical properties of this type of cluster is provided. Our results on the X = halogen series are compared to previous HF data on related compounds from Vitale et al.[5a,d]

* Author to whom correspondence should be addressed. E-mail: saillard@univ-rennes1.fr.

† This article is dedicated to our friend Professor David Carrillo (PUC, Valparaiso) on the occasion of his 65th birthday.

‡ Université de Rennes 1.

§ Universidad de Chile.

|| Present address: Departamento de Química, Facultad de Ciencias, Universidad de Tarapacá, Av. General Velásquez 1775, Arica, Chile. E-mail: anvega@dfi.uchile.cl.

(1) See for example: Cotton, F. A.; Wilkinson, G. *Advanced Inorganic Chemistry: A Comprehensive Text*, 4th ed.; John Wiley & Sons: New York, 1980; p 800.

(2) Mehrotra, P. K.; Hoffmann, R. *Inorg. Chem.* **1978**, *17*, 2187.

(3) (a)Pyykkö, P. *Chem. Rev.* **1997**, *97*, 597. (b) Pyykkö, P.; Mendizabal, F. *Inorg. Chem.* **1998**, *37*, 3018.

(4) (a) Garland, M. T.; Halet, J.-F.; Saillard, J.-Y. *Inorg. Chem.* **2001**, *40*, 3342. (b) Vega, A.; Calvo, V.; Zárate, A.; Fuenzalida, V.; Saillard, J.-Y. *Inorg. Chem.* **2002**, *41*, 3389. (c) Moreno, Y.; Spodine, E.; Vega, A.; Saillard, J.-Y. *Inorg. Chim. Acta* **2003**, *350*, 651.

(5) (a) Vitale, M.; Palke, W. E.; Ford, P. C. *J. Phys. Chem.* **1992**, *96*, 8329. (b) Ryu, C. K.; Vitale, M.; Ford, P. C. *Inorg. Chem.* **1993**, *32*, 869. (c) Ford, P. C.; Vogler, A. *Acc. Chem. Res.* **1993**, *26*, 220. (d) Vitale, M.; Ryu, C. K.; Palke, W. E.; Ford, P. C. *Inorg. Chem.* **1994**, *33*, 561. (e) Tran, D.; Bourassa, J. L.; Ford, P. C. *Inorg. Chem.* **1997**, *36*, 439. (f) Ford, P. C. *Coord. Chem. Rev.* **1994**, *132*, 129. (g) Ford, P. C.; Cariati, E.; Bourassa, J. *Chem. Rev.* **1999**, *99*, 3626.

10.1021/ic035262r CCC: $27.50
Published on Web 05/20/2004

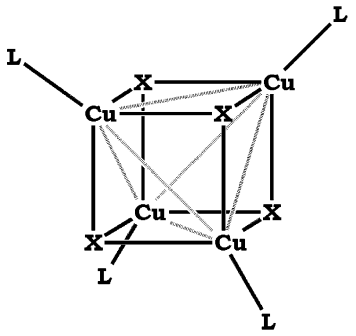

Figure 1. Typical tetrahedral structure of a $Cu_4(\mu_3\text{-}X)_4L_4$ complex.

Computational Details

DFT[6] calculations were carried out using the Amsterdam Density Functional (ADF) program.[7] The Vosko−Wilk−Nusair parametrization[8] was used to treat electron correlation within the local density approximation, with gradient corrections added for exchange (Becke88)[9] and correlation (Perdew).[10] The numerical integration procedure applied for the calculations was developed by te Velde and Baerends.[6d]

The standard ADF TZP basis set was used for the all the atoms: a triple-ξ Slater-type orbital (STO) basis set for valence orbitals plus a polarization single-ξ STO. Relativistic corrections were added by the use of the ZORA (zeroth order regular approximation) scalar Hamiltonian in the case of the iodine compounds.[11] The frozen core approximation was used to treat core electrons.[6d] Full geometry optimizations were carried out on each complex using the analytical gradient method, implemented by Verluis and Ziegler.[12] Unless specified in the text, T_d symmetry was used as a constraint in all the geometry optimizations. The most stable rotational conformer of the molecules, corresponding to the N−H (or P−H) bonds eclipsing the Cu−X bonds, was considered.

Fragment interaction analysis between $Cu_4(L)_4^{4+}$ and X_4^{4-} was done using the method proposed by Ziegler.[13] Using this approach, the orbital interaction energy was decomposed into components associated with the various irreducible representations of the T_d symmetry group. Since the $4a_1$ orbital of the $Cu_4(L)_4^{4+}$ fragment was very close in energy to the d-block (and sometimes within), the electron configuration of this fragment was forced to be $4a_1^0 7t_2^0$ (see Figure 2) in all cases.

Results and Discussion

Survey of the Available Structural X-ray Data of $Cu_4(\mu_3\text{-}X)_4L_4$ Clusters. A search on the Cambridge Structural Database (CSD)[14] yielded 62 crystal structures of $Cu_4(\mu_3\text{-}X_4)L_4$ clusters, in which X is an alkynyl, a halogen, or an alkoxy ligand and L is a two-electron ligand.[15−60] Their major internuclear distances are listed in Table 1. All the

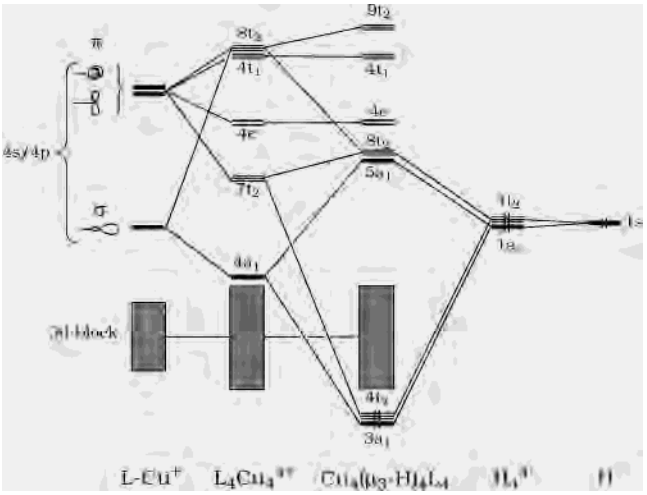

Figure 2. Simplified interaction MO diagram for a $Cu_4(\mu_3\text{-}H)_4L_4$ cluster (L = neutral, two-electron ligand).

(6) (a) Baerends, E. J.; Ellis, D. E.; Ros, P. *Chem. Phys.* **1973**, *2*, 41. (b) Baerends, E. J.; Ross, P. *Int. J. Quantum Chem.* **1978**, *S12*, 169. (c) Boerrigter, P. M.; te Velde, G. Baerends, E. J. *Int. J. Quantum Chem.* **1988**, *33*, 87. (d) te Velde, G.; Baerends, E. J. *J. Comput. Phys.* **1992**, *99*, 84.

(7) *Amsterdam Density Functional (ADF) program, version 2.3*; Vrije Universiteit: Amsterdam, Netherlands, 1997.

(8) Vosko, S. D.; Wilk, L.; Nusair, M. *Can. J. Chem.* **1990**, *58*, 1200.

(9) (a) Becke, A. D. *J. Chem. Phys.* **1986**, *84*, 4524. (b) Becke, A. D. *Phys. Rev. A: At., Mol., Opt. Phys.* **1988**, *38*, 2098.

(10) (a) Perdew, J. P. *Phys. Rev. B: Condens. Matter Mater. Phys.* **1986**, *33*, 8882. (b) Perdew, J. P. *Phys. Rev. A: At., Mol., Opt. Phys.* **1986**, *34*, 7406.

(11) (a) van Lenthe, E.; Baerends, E. J.; Snijders, J. G. *J. Chem. Phys.* **1993**, *99*, 4597. (b) van Lenthe, E.; Baerends, E. J.; Snijders, J. G. *J. Chem. Phys.* **1994**, *101*, 9783. (c) van Lenthe, E.; van Leeuwen, R.; Baerends, E. J. *Int. J. Quantum Chem.* **1996**, *57*, 281.

(12) Verluis, L.; Ziegler, T. *J. Chem. Phys.* **1988**, *88*, 322.

(13) Ziegler, T. In *Metal Ligand Interactions: From Atoms to Clusters to Surfaces*; Salahub, D. R., Russo, N., Eds.; Kluwer: Dordrecht, 1992; p 367.

(14) *Cambridge Structural Data Base*. Cambridge Crystallographic Data Center, Version 5.20.

(15) Naldini, L.; Demartin, F.; Manassero, M.; Sansoni, M.; Rassu, G.; Zoroddu, M. A. *J. Organomet. Chem.* **1985**, *279*, C42.

(16) Gamasa, M. P.; Gimeno, J.; Lastra, E.; Solans, X. *J. Organomet. Chem.* **1988**, *346*, 277.

(17) Yam, V. W.; Lee, W.-K.; Cheung, K.-K. *J. Chem. Soc., Dalton Trans.* **1996**, 2335.

(18) Yam, V. W.; Fung, W. K.; Cheung, K.-K. *J. Cluster Sci.* **1999**, *10*, 37.

(19) Yam, V. W.; Lam, C.-H.; Zhu, N. *Inorg. Chim. Acta* **2002**, *331*, 239.

(20) Osakada, K.; Takizawa, T.; Yamamoto, T. *Organometallics* **1995**, *14*, 3531.

(21) Dyason, J. C.; Healy, P. C.; Engelhardt, L. M.; Pakawatchai, C.; Patrick, V. A.; Raston, C. L.; White, A. H. *J. Chem. Soc., Dalton Trans.* **1985**, 831.

(22) Engelhardt, L. M.; Healy, P. C.; Kildea, J. D.; White, A. H. *Aust. J. Chem.* **1989**, *42*, 107.

(23) Churchill, M. R.; De Boer, B. G.; Mendak, S. J. *Inorg. Chem.* **1975**, *14*, 2041.

(24) Bottcher, H.-C.; Graf, M.; Merzweiler, K.; Bruhn, C. *Polyhedron* **1997**, *16*, 3253.

(25) Stolmar, M.; Floriani, C.; Gervasio, G.; Viterbo, D. *J. Chem. Soc., Dalton Trans.* **1997**, 1119.

(26) Pike, R. D.; Starnes, W. H., Jr.; Carpenter, G. B. *Acta Crystallogr., Sect. C: Cryst. Struct. Commun.* **1999**, *C55*, 162.

(27) Clayton, W. R.; Shore, S. G. *Cryst. Struct. Commun.* **1973**, *2*, 605.

(28) Churchill, M. R.; Kalra, K. L. *Inorg. Chem.* **1974**, *13*, 1065.

(29) Hakansson, M.; Jagner, S. *J. Organomet. Chem.* **1990**, *397*, 383.

(30) Hakansson, M.; Jagner, S.; Clot, E.; Eisenstein, O. *Inorg. Chem.* **1992**, *31*, 5389.

(31) Schramm, V. *Cryst. Struct. Commun.* **1980**, *9*, 1231.

(32) Goel, R. G.; Beauchamp, A. L. *Inorg. Chem.* **1983**, *22*, 395.

(33) Barron, P. F.; Dyason, J. C.; Engelhardt, L. M.; Healy, P. C.; White, A. H. *Inorg. Chem.* **1984**, *23*, 3766.

(34) Nifantyev, E. E.; Teleshev, A. T.; Blokhin, Y. I.; Antipin, M. Y.; Struchkov, Y. T. *Zh. Obshch. Khim.* **1985**, *55*, 1265.

(35) Nifantyev, E. E.; Koroteev, M. P.; Koroteev, A. M.; Belsky, V. K.; Stash, A. I.; Antipin, M. Y.; Lysenko, K. A.; Cao, L. *J. Organomet. Chem.* **1999**, *587*, 18.

(36) Kukhareva, T. S.; Vasyanina, L. K.; Antipin, M. Y.; Lyssenko, K. A.; Nifantev, E. E.; Soboleva, N. O. *Zh. Obshch. Khim.* **2001**, *71*, 551.

(37) Kataeva, O. N.; Krivolapov, D. B.; Gubaidullin, A. T.; Litvinov, I. A.; Kursheva, L. I.; Katsyuba, S. A. *J. Mol.Struct.* **2000**, *554*, 127.

(38) Zheng, H.-G.; Jin, Q.-H.; Xin, X.-Q.; Yu, K.-B. *Chin. J. Struct. Chem.* **2001**, *20*, 124.

(39) Bowmaker, G. A.; Effendy, H.; Hart, R. D.; Kildea, J. D.; White, A. H. *Aust. J. Chem.* **1997**, *50*, 653.

Table 1. Selected Averaged Geometrical Parameters for Structurally-Characterized $Cu_4(\mu_3\text{-}X)_4L_4$ Complexes. The Ranges Are Given in Parentheses

X	L[i]	Cu−Cu	Cu−X	Cu−L	ref
CCPh	PPh_3	2.606(2.523−2.676)	2.185(2.072−2.380)	2.228(2.221−2.234)	15
CCPh	PPh_2Py	2.639(2.594−2.686)	2.171(2.053−2.346)	2.231(2.220−2.241)	16
CCPh	$P(p\text{-Tol})_3$	2.588(2.567−2.606)	2.174(2.109−2.288)	2.239(2.219−2.257)	17
CC*p*-An	PPh_3	2.594(2.524−2.663)	2.171(2.119−2.265)	2.237(2.227−2.253)	18
CCCCPh	PPh_3	2.614(2.532−2.694)	2.156(2.064−2.248)		19
$CCSiMe_3$[a]	PPh_3	2.592(2.544−2.642)	2.170(2.119−2.235)	2.242(2.225−2.253)	20
$CCSiMe_3$[b]	PPh_3	2.576(2.566−2.576)	2.148(2.132−2.168)	2.231(2.226−2.244)	20
Average		2.601	2.168	2.235	
Cl	NEt_3	3.065(3.065−3.065)	2.439(2.439−2.439)	2.056(2.056−2.056)	21
Cl	Tmspy	3.077(2.960−3.194)	2.490(2.225−2.635)	1.986(1.986−1.986)	21
Cl	dppy	2.894(2.879−2.901)	2.454(2.250−2.599)	1.994(1.994−1.994)	22
Average		3.012	2.461	2.012	
Cl	PEt_3	3.211(3.211−3.211)	2.438(2.438−2.438)	2.176(2.176−2.176)	23
Cl	$PH(t\text{-Bu})_2$	3.307(3.230−3.376)	2.449(2.382−2.532)	2.191(2.187−2.194)	24
Cl	PGf_3	3.308(3.225−3.359)	2.437(2.382−2.465)	2.157(2.157−2.157)	25
Cl	$P(OPh)_3$	3.291(3.227−3.391)	2.426(2.356−2.531)	2.156(2.148−2.166)	26
Cl	PPh_3	3.303(3.112−3.424)	2.438(2.353−2.502)	2.190(2.185−2.194)	27
Cl	PPh_3	3.309(3.119−3.439)	2.445(2.363−2.505)	2.191(2.169−2.192)	28
Average		3.288	2.439	2.177	
Cl[c]	Dcp	3.331(3.177−3.546)	2.607(2.275−3.015)		29
Cl[d]	Dcp	3.264(3.016−3.532)	2.483(2.284−2.852)		29
Cl	Diene	3.451(3.263−3.784)	2.521(2.264−2.095)		30
Average		3.349	2.537		
Br	NEt_3	3.040(3.040−3.040)	2.537(2.537−2.537)	2.061(2.061−2.061)	21
Br	Pic	2.911(2.835−3.033)	2.540(2.435−2.623)	2.057(2.055−2.059)	31
Br	Dppy	2.878(2.870−2.893)	2.546(2.425−2.625)	2.024(2.024−2.024)	22
Average		2.943	2.541	2.047	
Br	PEt_3	3.184(3.184−3.184)	2.544(2.544−2.544)	2.199(2.199−2.199)	23
Br	$P(t\text{-Bu})_3$	3.485(3.479−3.491)	2.593(2.571−2.604)	2.228(2.228−2.228)	32
Br	PPh_3	3.345(3.087−3.541)	2.555(2.490−2.617)	2.208(2.206−2.209)	33
Br	$P(OPh)_3$	3.294(3.265−3.323)	2.562(2.447−2.749)	2.160(2.145−2.165)	26
Br	Dioxa	3.325(3.288−3.399)	2.540(2.467−2.644)	2.177(2.174−2.179)	34
Br	Gffph	3.190(3.114−3.297)	2.522(2.458−2.586)	2.159(2.154−2.166)	35
Br	Phosph	3.276(3.157−3.373)	2.546(2.470−2.720)	2.166(2.162−2.176)	36
Br	$P(Si\text{-Pr})_3$	3.183(3.126−3.296)	2.527(2.456−2.582)	2.203(2.182−2.231)	37
Br	$P(p\text{-An})_3$	3.288(3.212−3.265)	2.542(2.466−2.634)	2.202(2.198−2.203)	38
Average		3.285	2.548	2.189	
Br	Dcp	3.484(3.484−3.484)	2.648(2.396−3.116)		30
Br	$AsPh_3$	3.267(3.197−3.322)	2.521(2.452−2.600)	2.321(2.318−2.324)	39
I	NMe_3	2.688(2.677−2.735)	2.687(2.678−2.689)	2.109(2.091−2.127)	40
I	Pip	2.657(2.630−2.651)	2.701(2.691−2.717)	2.053(2.053−2.053)	41
I	Py	2.690(2.619−2.721)	2.703(2.630−2.794)	2.041(2.024−2.051)	42
I	Pic	2.720(2.673−2.754)	2.698(2.629−2.773)	2.010(1.897−2.075)	43
I	3-pic	2.686(2.618−2.746)	2.693(2.640−2.722)	2.045(1.990−2.081)	44
I	3-pic	2.706(2.647−2.739)	2.717(2.665−2.781)	2.043(2.035−2.061)	45
I	4-pic	2.694(2.652−2.736)	2.693(2.671−2.714)	2.031(2.031−2.031)	45
I	Dppy	2.917(2.870−3.010)	2.686(2.639−2.726)	2.066(2.066−2.066)	22
I	DPS[j]	2.657(2.618−2.696)	2.673(2.634−2.727)	2.023(2.019−2.027)	46
I	DPS[k]	2.659(2.602−2.702)	2.704(2.596−2.950)	2.027(2.018−2.033)	46
I	NNP	2.719(2.640−2.844)	2.693(2.648−2.728)	2.046(2.035−2.060)	47
I	SiL	2.689(2.617−2.824)	2.698(2.652−2.765)	2.042(2.032−2.051)	48
I	$NADEt_2$	2.665(2.630−2.696)	2.696(2.630−2.749)	2.036(2.028−2.043)	49
I	Pyrrpy	2.703(2.675−2.734)	2.699(2.644−2.764)	2.036(2.018−2.049)	50
I	Bzim	2.746(2.740−2.757)	2.699(2.687−2.720)	2.029(2.029−2.029)	51
I	MeCN	2.771(2.726−2.846)	2.694(2.630−2.751)	2.000(1.990−2.009)	52
Average		2.710	2.696	2.040	
I	PEt_3	2.927(2.927−2.927)	2.684(2.684−2.684)	2.254(2.254−2.254)	53
I	$P(Nme_3)_3$	3.386(3.283−3.465)	2.726(2.697−2.754)	2.231(2.229−2.235)	54
I	PPh_2Me	2.930(2.840−3.010)	2.698(2.611−2.759)	2.250(2.250−2.250)	55
I	PPh_3	2.968(2.839−3.165)	2.691(2.653−2.732)	2.252(2.242−2.258)	21
I	DMPP	2.920(2.829−3.056)	2.683(2.635−2.730)	2.254(2.252−2.255)	56
I	Fccx	3.071(2.865−3.209)	2.692(2.617−2.756)	2.248(2.240−2.255)	57
Average		3.034	2.696	2.248	

Table 1 (Continued)

X	L[i]	Cu−Cu	Cu−X	Cu−L	ref
I	$AsEt_3$	2.782(2.782−2.782)	2.677(2.677−2.677)	2.361(2.361−2.361)	53
I[e]	$AsPh_3$	2.834(2.793−2.900)	2.688(2.667−2.703)	2.374(2.366−2.384)	58
I[f]	$AsPh_3$	2.772(2.672−2.890)	2.681(2.663−2.711)	2.359(2.350−2.368)	39
I[g]	$AsPh_3$	2.820(2.727−2.894)	2.690(2.666−2.701)	2.373(2.368−2.372)	39
I[h]	$AsPh_3$	2.886(2.834−2.936)	2.684(2.657−2.718)	2.376(2.371−2.383)	39
Average		2.819	2.684	2.369	
OPh	PPh_3	3.181(3.125−3.260)	2.140(2.050−2.260)	2.147(2.130−2.152)	59
O*t*-Bu	CO	3.040(3.036−3.043)	2.063(2.063−2.063)	1.776(1.768−1.783)	60

[a] Polymorph I. [b] Polymorph II. [c] Tetragonal polymorph. [d] Orthorhombic polymorph. [e] Polymorph α. [f] Polymorph *β*. [g] Polymorph *γ*. [h] Polymorph *δ*. [i] Ph = C_6H_5; Py = C_5H_5N; *p*-Tol$_3$ = *p*-$C_6H_4CH_3$; *p*-An = *p*-$C_6H_4OCH_3$; Me = CH_3; Et = C_2H_5; Tmspy = 2-$((CH_3)_3Si)_2CH-C_5H_4N$; dppy = 2-$(C_6H_5)_2CH-C_5H_4N$; *t*-Bu = $C(CH_3)_3$; Gf = P(1,2:5,6-di-*O*-isopropylidene-α-D-glucofuranoside)$_3$; Dcp = *endo*-dicyclopentadiene; diene = 1,4-pentadiene; pic = 2-methylpyridine; dioxa = (2-diethylamino-5,5-dimethyl-1,3,2-dioxaphosphorinan-2-yl); Gffph = 1,2-*O*-isopropylidene-α-D-glucofuranose 3,5,6-bicyclophosphite; Phosph = 2-ethoxy-5,5-dimethyl-1,3,2-dioxaphosphorinane; Si-Pr = thioisopropyl; pip = $C_5H_{10}NH$; 3-pic = 3-methyl-pyridine; 4-pic = 4-methyl-pyridine; DPS = bis(pyrid-4-yl)disulfide; NNP = 3-(4,4,5,5-tetramethyl-4,5-dihydro-1*H*-imidazolyl-1-oxyl-3-oxide)pyridine; SiL = 1,1,3,3-tetra-isopropyl-1,3-bis((pyrid-3-yl)oxy)disiloxane; $NADEt_2$ = *N*,*N*-diethylnicotinamide; pyrrpy = 3-(pyrrolylmethyl)pyridine; bzim = benzimidazole; DMPP = 1-phenyl-3,4-dimethylphosphole; Fccx = (1′-diphenylphosphino)ferrocenecarboxylic acid. [j] Propionitrile solvate. [k] Acetonitrile solvate.

reported distances correspond to the CSD values.[14] When no data were available from CSD, the values published in the corresponding referenced papers were used. $Cu_4(\mu_3\text{-}X)_4L_4$ compounds with more than one kind of X or L ligand are not considered in Table 1. The structures are averaged with respect to the nature of X and L atom(s) bonded to Cu (nitrogen, phosphorus, arsenic, η^2-C_2). All the structures exhibit the tetrahedral arrangement depicted in Figure 1. Although some of these compounds have exact T_d symmetry, most of them have only approximate T_d symmetry. In particular, the dispersion of the Cu···Cu distances within several individual compounds is significant, the largest range (0.32 Å) being observed for X = I and L = Fccx.[57] Some dispersion of the averaged Cu···Cu distances within families of similar compounds is also present, the largest range (0.47 Å) corresponding to X = I and L = phosphine.[53−57] This dispersion of chemically equivalent Cu···Cu distances in Cu(I) clusters is quite common.[4a] It is indicative of a weak attractive potential between the metal centers, which is, consequently, very sensitive to steric and crystal packing effects. This dispersion is probably one of the causes of the unsymmetrical bridging of the μ_3-X ligands observed in some of the listed compounds (see Cu−X distances in Table 1). In the case of X = CCR, however, the particularly large dispersion of the Cu−X distances observed for some of the listed compounds[15−20] suggests that other effects, such as some π effect, could be at work. From this point of view, it is interesting to note that unsymmetrical bridging of μ_3-alkynyl ligands is also present in other types of Cu(I) clusters.[61] On the other hand, all the alkynyl compounds listed in Table 1 have their CC distances ranging from 1.179 to 1.241 Å. Their averaged value (1.203 Å) is not significantly different from that of a triple bond (1.20 Å).[62] This suggests that the π-type system of the alkynyl ligand is weakly involved in the bonding with the metal core and that CCR^- is better described as a two-electron rather than a six-electron ligand. When X^- is a halide (potentially a six-electron ligand), the Cu···Cu distances are significantly longer than for $X^- = CCR^-$. For the same halogen, they are, on average, ∼0.3 Å longer when L is a P-ligand than when it is an N-ligand. In the case of L = N-ligand, the average Cu···Cu distances are close for X = Cl and Br but significantly shorter (by ∼0.2 Å) for X = I. A similar trend is found in the case of L = P-ligand (Table 1).

In the following, we investigate the bonding in the compounds of Table 1 by analyzing the electronic structure of models in which the various N- and P-ligands are replaced by NH_3 and PH_3, respectively. Although such a simplification is expected to perturb somewhat the electronic structure and the HOMO and LUMO nature of each individual compound, it allows a general overview of the bonding and properties within a large series of compounds bearing X ligands of fairly different nature.

(40) Babich, O. A.; Kokozay, V. N. *Polyhedron* **1997**, *16*, 1487.
(41) Schramm, V. *Inorg. Chem.* **1978**, *17*, 714.
(42) Raston, C. L.; White, A. H. *J. Chem. Soc., Dalton Trans.* **1976**, 2153.
(43) Healy, P. C.; Pakawatchai, C.; Raston, C. L.; Skelton, B. W.; White, A. H. *J. Chem. Soc., Dalton Trans.* **1983**, 1905.
(44) Schramm, V. *Cryst. Struct. Commun.* **1982**, *11*, 1549.
(45) Cariati, E.; Bu, X.; Ford, P. C. *Chem. Mater.* **2000**, *12*, 3385.
(46) Blake, A. J.; Brooks, N. R.; Champness, N. R.; Crew, M.; Deveson, A.; Fenske, D.; Gregory, D. H.; Hanton, L. R.; Hubberstey, P.; Schroder, M. *Chem. Commun.* **2001**, 1432.
(47) Zhang, D.; Ding, L.; Xu, W.; Jin, X.; Zhu, D. *Chem. Lett.* **2001**, 242.
(48) Goodgame, D. M. L.; Lickiss, P. D.; Rooke, S. J.; White, A. J. P.; Williams, D. J. *Inorg. Chim. Acta* **2001**, *324*, 218.
(49) Churchill, M. R.; Davies, G.; El-Sayed, M. A.; Hutchinson, J. P.; Rupich, M. W. *Inorg. Chem.* **1982**, *21*, 995.
(50) Sugahara, E.; Paula, M. M. S.; Vencato, I.; Franco, C. V. *J. Coord. Chem.* **1996**, *39*, 59.
(51) Toth, A.; Floriani, C.; Chiesi-Villa, A.; Guastini, C. *Inorg. Chem.* **1987**, *26*, 3897.
(52) Jasinski, J. P.; Rath, N. P.; Holt, E. M. *Inorg. Chim. Acta* **1985**, *97*, 91.
(53) Churchill, M. R.; Kalra, K. L. *Inorg. Chem.* **1974**, *13*, 1899.
(54) Arkhireeva, T. M.; Bulychev, B. M.; Sizov, A. I.; Sokolova, T. A.; Belsky, V. K.; Soloveichik, G. L. *Inorg. Chim. Acta* **1990**, *169*, 109.
(55) Churchill, M. R.; Rotella, F. J. *Inorg. Chem.* **1977**, *16*, 3267.
(56) Attar, S.; Bowmaker, G. A.; Alcock, N. W.; Frye, J. S.; Bearden, W. H.; Nelson, J. H. *Inorg. Chem.* **1991**, *30*, 4743.
(57) Stepnicka, P.; Gyepes, R.; Podlaha, J. *Collect. Czech. Chem. Commun.* **1998**, *63*, 64.
(58) Churchill, M. R.; Youngs, W. J. *Inorg. Chem.* **1979**, *18*, 1133.
(59) Lopes, C.; Hakansson, M.; Jagner, S. *Inorg. Chim. Acta* **1997**, *254*, 361.
(60) Geerts, R. L.; Huffman, J. C.; Folting, K.; Lemmen, T. H.; Caulton, K. G. *J. Am. Chem. Soc.* **1983**, *105*, 3503.
(61) See for example: Yam, V. W.-W.; Lo, K. K.-W.; Wong K. M.-C. *J. Organomet. Chem.* **1999**, *578*, 3.
(62) Emsley, J. *The Elements*; Oxford University Press: New York, 1989.

Table 2. Major DFT Computed Data for $Cu_4(\mu_3\text{-}X)_4(LH_3)_4$ Complexes[a]

	L = NH_3						
	H	CH_3	CCH	F	Cl	Br	I
Cu···Cu	2.498	2.448	2.610	3.152	2.892	3.057	2.649
Cu−X	1.845	2.452	2.194	2.169	2.499	2.644	2.874
Cu−L	2.121	2.131	2.111	1.997	2.108	2.102	2.117
C−C			1.239				
Cu···H		2.743					
Pauli repulsion (eV)	41.80	19.65	40.82	20.92	27.82	26.49	22.23
electrostatic interaction (eV)	−96.20	−72.93	−77.43	−77.65	−75.78	−72.72	−68.95
"steric" interaction energy (eV)	−47.45	−43.68	−35.52	−56.98	−46.77	−44.67	−44.83
decomposition of the orbital interaction energy:							
A_1 orbital interaction energy (eV)	−22.79	−16.19	−20.85	−10.25	−12.11	−10.89	−10.61
A_2 orbital interaction energy (eV)	0.00	0.00	0.00	0.00	0.00	0.00	0.00
E orbital interaction energy (eV)	−0.49	−1.22	−2.69	−1.86	−1.60	−1.64	−1.14
T_1 orbital interaction energy (eV)	−0.83	−1.51	−3.00	−1.72	−1.58	−1.67	−1.11
T_2 orbital interaction energy (eV)	−10.39	−11.97	−11.71	−7.30	−6.62	−6.80	−5.81
total orbital interaction energy (eV)	−34.50	−30.90	−38.26	−21.12	−21.91	−21.00	−18.67
total bonding energy (eV)	−81.95	−74.58	−73.78	−78.10	−68.68	−65.66	−63.50
HOMO−LUMO gap (eV)	2.05	1.67	2.81	1.76	2.26	2.35	2.38
	L = PH_3						
	H	CH_3	CCH	F	Cl	Br	I
Cu···Cu	2.531	2.493	2.618	3.160	2.857	2.894	2.998
Cu−X	1.855	2.401	2.179	2.140	2.475	2.622	2.830
Cu−L	2.253	2.253	2.275	2.165	2.285	2.304	2.315
C−C			1.236				
Cu···H		2.676					
Pauli repulsion (eV)	37.52	21.24	37.25	19.72	27.46	26.62	24.60
electrostatic interaction (eV)	−92.82	−73.22	−74.92	−76.11	−73.04	−69.68	−67.11
"steric" interaction energy (eV)	−48.75	−42.64	−37.51	−56.88	−45.60	−42.94	−42.14
decomposition of the orbital interaction energy:							
A_1 orbital interaction energy (eV)	−18.70	−13.61	−15.80	−8.93	−10.84	−10.37	−9.67
A_2 orbital interaction energy (eV)	0.00	0.00	0.00	0.00	0.00	0.00	0.00
E orbital interaction energy (eV)	−0.57	−1.54	−3.25	−2.53	−1.98	−1.96	−1.61
T_1 orbital interaction energy (eV)	−1.01	−1.84	−3.54	−2.49	−2.02	−2.01	−1.59
T_2 orbital interaction energy (eV)	−13.24	−15.08	−13.67	−9.54	−8.41	−8.27	−7.42
total orbital interaction energy (eV)	−33.52	−32.08	−36.25	−23.50	−23.25	−22.55	−20.30
total bonding energy (eV)	−82.28	−74.72	−73.77	−80.39	−68.85	−65.49	−62.45
HOMO−LUMO gap (eV)	2.91	3.10	3.68	3.55	3.30	3.15	3.26

[a] The bonding energy refers to the $Cu_4(LH_3)_4^{4+}$ and X_4^{4-} fragments.

Bonding Analysis of the Models $Cu_4(\mu_3\text{-}X)_4L_4$ (X = H, CH_3, CCH, F, Cl, Br, I; L = NH_3, PH_3). The major computed data for the model series $Cu_4(\mu_3\text{-}X)_4L_4$ (X = H, CH_3, CCH, F, Cl, Br, I; L = NH_3, PH_3) are given in Table 2.

$Cu_4(\mu_3\text{-}H)_4L_4$. To analyze the effect of the ligand electron count on the structure of the studied clusters, we start our analysis with the case of X^- = hydride, a pure two-electron σ-type ligand. To our knowledge, there is no report so far in the literature of a hydride compound of the type $Cu_4(\mu_3\text{-}H)_4L_4$. The optimized Cu···Cu distance is shorter in the case of L = NH_3 than with L = PH_3. To understand this situation, one has to consider the interaction between the $L_4Cu_4^{4+}$ and H_4^{4-} tetrahedral fragments, which is illustrated by the interaction molecular orbital (MO) diagram sketched in Figure 1. The H_4^{4-} tetrahedral fragment has four occupied frontier orbitals of a_1 and t_2 symmetry in T_d symmetry. They are all nonbonding combinations of 1s(H) AOs, since there is no significant H···H contact (see right side of Figure 1). A single L−Cu^+ unit exhibits three vacant orbitals of 4s and 4p dominant character, which lie above the five 3d orbitals that are occupied (see left side of Figure 1). When four L−Cu^+ units are brought together to form the $L_4Cu_4^{4+}$ tetrahedral fragment, the contracted 3d orbitals overlap weakly, giving rise to a more or less nonbonding 3d-block. On the other hand, the σ-type 4s/4p hybrids overlap significantly, leading to bonding ($4a_1$) and antibonding ($8t_2$) combinations. Similarly, the σ-type 4p AOs give rise to weakly bonding ($7t_2$), nonbonding (4e), and weakly antibonding ($4t_1$) combinations (see left side of Figure 1). Some mixing between the $7t_2$ and $8t_2$ levels (not illustrated in Figure 1) tends to increase the bonding nature of $7t_2$. When the $L_4Cu_4^{4+}$ and H_4^{4-} fragments are put together to form the $Cu_4(\mu_3\text{-}H)_4L_4$ cluster, only orbitals of a_1 and t_2 symmetry can interact, giving rise to the occupied bonding $3a_1$ and $4t_2$ levels and to the vacant $5a_1$ and $8t_2$ levels shown in the middle of Figure 1. The $9t_2$ level of $Cu_4(\mu_3\text{-}H)_4L_4$ also has some Cu−X antibonding character. The mixing of Cu···Cu bonding $4a_1$ (mainly) and $7t_2$ (secondarily) empty levels of $L_4Cu_4^{4+}$ into the occupied $3a_1$ and $4t_2$ MOs of $Cu_4(\mu_3\text{-}H)_4L_4$

tends to reinforce Cu···Cu bonding, while the mixing of the $8t_2$ level of $L_4Cu_4^{4+}$ into occupied orbitals of $Cu_4(\mu_3\text{-}H)_4L_4$ tends to weaken Cu···Cu bonding, but to a lesser extent due to its separation in energy from the H_4^{4-} frontier orbitals. This is supported by the comparison of the optimized Cu···Cu distances in $Cu_4(\mu_3\text{-}H)_4(NH_3)_4$ and $[(NH_3)_4Cu_4]^{4+}$, which are 2.498 and 3.004 Å, respectively.

The ADF program provides the opportunity to carry out an analysis of the interaction between the $L_4Cu_4^{4+}$ and H_4^{4-} fragments in the $Cu_4(\mu_3\text{-}H)_4L_4$ clusters by using the method of decomposition of the bonding energy between fragments proposed by Ziegler.[13] In this method, the bonding energy between the geometrically unrelaxed fragments is broken down into three terms: an electrostatic term, a Pauli repulsion term, and an orbital interaction term. The Pauli repulsion term is generally approximated to the sum of the four-electron/two-orbital destabilizations, while the orbital interaction term is approximated to the two-electron/two-orbital stabilizations. The sum of the electrostatic and Pauli repulsion terms is generally called the "steric" interaction energy. Moreover, the orbital interaction energy can be broken down into components associated with the various irreducible representations of the molecule symmetry group. The energy decomposition terms of the computed $Cu_4(\mu_3\text{-}H)_4L_4$ models are given in Table 2. The total bonding energy between both tetrahedral fragments indicates stronger bonding in the case of L = PH_3. This is due to a much lower Pauli repulsion in the latter case. Indeed, the orbital interaction component of the total energy is indicative of a stronger attractive interaction in the case of L = NH_3 because of its larger A_1 component. The result is a shorter Cu···Cu contact in the L = NH_3 case. On the other hand, the Cu−X distances are quite similar in both compounds, presumably as the result of a balance between the Pauli repulsion and orbital interaction terms.

Finally, one should not be surprised that the breakdown of the orbital interaction energy of both $Cu_4(\mu_3\text{-}H)_4L_4$ clusters contains small, but nonzero, E and T_1 terms. They originate from the presence of hydrogen 2p polarization orbitals in the considered basis set.

$Cu_4(\mu_3\text{-}CH_3)_4L_4$. Methyl is a weak π-donor ligand. Indeed, it possesses occupied σ(C−H) combinations, which are of π-type symmetry with respect to the CH_3 symmetry axis.[63] The existence of such π-donating orbitals on the X^- ligand leads to the formation of occupied combinations of e, t_1, and t_2 symmetry on the X_4^{4-} fragment, in addition to the a_1 and t_2 σ-type combinations shown in Figure 2. These π-type combinations are susceptible to interact in a stabilizing way with the 4e, $4t_1$, $7t_2$, and $8t_2$ frontier orbitals of the $L_4Cu_4^{4+}$ fragment (see left side of Figure 2). Calculations on the $Cu_4(\mu_3\text{-}CH_3)_4(NH_3)_4$ and $Cu_4(\mu_3\text{-}CH_3)_4(PH_3)_4$ models indicated important steric hindrance between the terminal and bridging ligands, which are minimized only with very long Cu−C distances (see Table 2). Some weak Cu···H agostic interaction is also present in these optimized models (see Table 2). Decomposition of the orbital interaction energy shows E and T_1 components which are weak but larger than those in $Cu_4(\mu_3\text{-}H)_4(PH_3)_4$. This is indicative of the weak π-donating ability of the CH_3 groups.

$Cu_4(\mu_3\text{-}CCH)_4L_4$. Geometry optimizations under T_d symmetry constraint lead to E and T_1 π-type orbital interaction terms which are not very large, although being roughly twice those computed for $Cu_4(\mu_3\text{-}CH_3)_4(PH_3)_4$ (Table 2). Again, the orbital interaction energy is dominated by the A_1 and T_2 components. The optimized distances of $Cu_4(\mu_3\text{-}CCH)_4(PH_3)_4$ are in good agreement with the X-ray data of related compounds (compare Tables 1 and 2). The optimized CC distance (~1.24 Å in both clusters) is slightly larger than that optimized with the same method for acetylene (1.208 Å), in agreement with some π-donation of the alkynyl ligands to the metals.

As mentioned above, the X-ray data of most of the alkynyl clusters exhibit unsymmetrical bridging of the μ_3-CCR ligands (see Table 1). Three different Cu−C bond distances (short, intermediate, and long) are often observed, with the CCR axis being always close to orthogonality with the Cu_3 plane to which it is bonded.[61] The optimization of $Cu_4[\mu_3\text{-}(CCH)_4](PH_3)_4$ in D_{2h} symmetry, which allows two types of Cu−C distances per CCH ligand, leads to two long (2.207 Å) and one short (2.135 Å) Cu−C distances. Interestingly, although significantly distorted, this structure is isoenergetic to the T_d one. Optimization with the C_1 symmetry leads to an average Cu···Cu distance of 2.630 Å, ranging from 2.579 to 2.648 Å. Cu−C distances vary from 2.148 to 2.231 Å. The C_1 model is only 0.03 eV less stable than the T_d one. It is noteworthy that the β carbon atom is not involved in the metal−CCR interaction. Therefore, the asymmetric bonding could be partly due to the existence of a better overlap of the σ- and/or π-type frontier orbital of the C_α alkenyl ligand. Nevertheless, the origin of the asymmetric bridging of the μ_3-CCR ligand results from the balance of several electronic and steric effects in such a way that the potential energy surface associated with the distortion away from symmetrical μ_3 bridging is very flat.[64] This problem is currently being investigated in more detail in our group on more simple models.

The $Cu_4(\mu_3\text{-}X)_4L_4$ (X = halogen) Series. The optimized metrical data corresponding to X = Cl, Br, and I (Table 2) differ to some extent from the reported X-ray structures of related compounds (Table 1). The optimized Cu−X distances are larger than the experimental ones, as is often the case with DFT calculations with gradient corrections.[4] More surprisingly, in several models, the optimized Cu···Cu distances are shorter than the averaged experimental ones. Moreover, the experimental trend for shorter Cu···Cu distances when X = I (see above) is not reproduced in the case of L = PH_3. This discrepancy with experiment is likely to be attributed to the failure of the gradient-corrected DFT method used in the calculations, which is known for not correctly taking into account dispersion energy between non-overlapping systems, especially in the case of the softer

(63) Libit, L.; Hoffmann, R. *J. Am. Chem. Soc.* **1974**, *96*, 1370.

(64) Yam, V. W.-W.; Lo, W.-Y.; Lam, S. C.-F.; Cheung, K.-K.; Zhu, N.; Fathallah, S.; Le Guennic, B.; Kahlal, S.; Halet, J.-F. *J. Am. Chem. Soc.*, **2004**, *126*, in press.

halogen ligands.[3a,65] Calculations at the HF/MP2 level have been proved to be more accurate in reproducing metal−metal distances in related compounds.[3d,65,66] It turns out that a test geometry optimization run on $Cu_4(\mu_3\text{-}I)_4(PH_3)_4$ at the HF/MP2 level led to a Cu···Cu separation of 2.754 Å, i.e. shorter than experiment (see Table 1).[67] At any rate, the much cheaper DFT calculations reproduce most of the trends within the X = halogen series so that they can be used safely for a qualitative orbital and bonding analysis.

The breakdown of the bonding energy between the $Cu_4L_4^{4+}$ and X_4^{4-} fragments (Table 2) shows that halides are weaker σ-donors than H^-, CH_3^-, or CCR^- and are weaker π-donors than CCR^-. Clearly, there is no strong π-donation in the halide series. Therefore, the Cu···Cu separation appears to be significantly dependent on the a_1 bonding interaction and, to a lesser extent, on the overall weakly antibonding t_2 interactions.

Our calculated ground-state electronic structures on this series are in a general qualitative agreement with previous single-point Hartree−Fock calculations carried out on related compounds by Vitale et al.,[5a,d] except for the composition of the highest occupied levels, which were found to have a dominant halogen character by these authors, whereas our calculations indicate a major Cu(3d) participation for the whole series (see below).

Nature of the HOMOs and LUMOs of the Computed Models. The HOMOs of the computed models are of t_2 symmetry, except for $Cu_4(\mu_3\text{-}F)_4(PH_3)_4$ where they are of t_1 symmetry. As for all the highest occupied orbitals, they have a dominant Cu(3d) character. The Cu and X participation to the HOMO indicates a larger X contribution for L = PH_3 than for L = NH_3. Within the halogen series, the Cu participation decreases when going from F to I, as expected from the variation of the valence AO energies within the series (from 87% to 72% in the case of L = NH_3 and from 85% to 48% in the case of L = PH_3). However, the halogen participation to the HOMO never exceeds 40% (where X = I and L = PH_3), a result at variance with previous Hartree−Fock calculations.[5a,d]

The LUMO of the $Cu_4(\mu_3\text{-}X)_4L_4$ clusters is found to be the $5a_1$ orbital of Figure 2 (except for L = PH_3 and X = H, CCH, where the LUMO is of e symmetry). The Cu participation to the cluster $5a_1$ MO depends on the energy of the σ-type frontier orbitals of X. The lower this energy, the larger the Cu···Cu bonding character in $5a_1$. Thus, in the case of X = H, CH_3, and CCH, the $5a_1$ MO never exceeds 25% of Cu participation, while in the case of the more electronegative halogens this participation varies from 59% (X = F) to 56% (X = I) when L = NH_3 and from 95% (X = F) to 73% (X = I) when L = PH_3. Populating the $5a_1$ MO is expected to shorten the Cu···Cu separation due to its Cu···Cu bonding character.[5] The larger the Cu participation in $5a_1$, the larger the shortening of the Cu···Cu distance in the excited state. This is what happens in the lower triplet excited state when the LUMO is $5a_1$. In the case of L = NH_3, the optimized Cu···Cu distances are 2.521, 2.481, 2.671, 2.741, 2.549, 3.130, and 2.534 Å for X = H, CH_3, CCH, F, Cl, Br, and I, respectively. In the case of L = PH_3, the corresponding values are 2.541, 2.503, 2.642, 3.104, 2.702, 2.647, and 2.588 Å, respectively. Therefore, the contraction of the Cu_4 tetrahedron in the triplet state is significant in most of the cases when X = halogen. It is also, to some extent, related to the nature of the HOMO, as exemplified by the smaller contraction computed for the X = F and L = PH_3 case, for which the HOMO is of a different symmetry from that of the other clusters (see above). This contraction effect has been proposed to rationalize the luminescence properties of some $Cu_4(\mu_3\text{-}X)_4L_4$ (X = halogen) compounds, especially in the case of X = I, for which the shortest Cu···Cu separations are observed. In particular, these compounds present large Stokes shifts, which are attributed to the variation of the Cu···Cu distances between the singlet ground state and the excited triplet state responsible for emission.[5]

Conclusion

DFT calculations on the $Cu_4(\mu_3\text{-}X)_4L_4$ series indicate that X-to-Cu π-donation remains small, regardless of the nature of X. Therefore, all the considered X^- ligands are better described as two-electron ligands, and the covalent part of the Cu···Cu bonding depends mainly upon the a_1 component of the σ-type interaction between the $L_4Cu_4^{4+}$ and X_4^{4-} fragments.

The first excited state corresponds to the occupation of a Cu···Cu bonding LUMO of a_1 symmetry, which is of dominant Cu(4s/4p) character when X is an electronegative ligand, such as a halogen. Consequently, this excited state is found to exhibit much shorter Cu···Cu distances than those of the ground state, as predicted by Ford and co-workers to rationalize the luminescence properties of related compounds.[5] However, in contrast to previous calculations carried out by these authors, the highest occupied orbitals are found to have a dominant Cu(3d) character, suggesting that the lowest transition is best described as corresponding to a $Cu_4(3d)\rightarrow Cu_4(s/p)$ charge transfer.

Acknowledgment. We thank Pr. A. Boucekkine for some computational help. A.V. is indebted to the CNRS (France) for a six-month grant and to the CIMAT (Chile) for a postdoctoral grant. Computing facilities were provided by the PCIO (Rennes), the IDRIS-CNRS (Orsay), and the CIMAT (Santiago). This work was also supported by a French−Chilean CNRS-CONICYT program (PICS 922).

IC035262R

(65) Wang, S.-G.; Schwarz, E. *J. Am. Chem. Soc.* **2004**, *126*, 1266.
(66) Hermann, H. L.; Boche, G.; Schwerdtfeger, P. *Chem. Eur. J.* **2001**, *7*, 5333.
(67) MP2 geometry optimization of $Cu_4(\mu_3\text{-}I)_4(PH_3)_4$ yielded Cu···Cu, Cu−I, and Cu−P distances of 2.754, 2.709, and 2.330 Å, respectively. In the triplet state, the corresponding value are 2.588, 2.806, and 2.264 Å, respectively (unpublished results).